Acta Crystallographica Section D
Biological Crystallography
ISSN 0907-4449

Crystallization of the Zα domain of the human editing enzyme ADAR1 complexed with a DNA–RNA chimeric oligonucleotide in the left-handed Z-conformation

Bernard A. Brown II,[a] Alekos Athanasiadis,[a] Eugene B. Hanlon,[b,c] Ky Lowenhaupt,[a] Christina M. Wilbert[a] and Alexander Rich[a]*

[a]Department of Biology, Massachusetts Institute of Technology, Cambridge, MA 02139, USA, [b]George R. Harrison Spectroscopy Laboratory, Massachusetts Institute of Technology, Cambridge, MA 02139, USA, and [c]Medical Research Service, Department of Veterans Affairs Medical Center, Bedford, Massachusetts, MA 01730, USA

Correspondence e-mail: cbeckman@mit.edu

Received 30 May 2001
Accepted 8 August 2001

The Zα domain of human double-stranded RNA adenosine deaminase (ADAR1) has been crystallized with a hexanucleotide containing alternating deoxyribose and ribose furanose sugars. Solution circular dichroism experiments show that this double-stranded chimera $(dCrG)_3$ initially adopts the right-handed A-conformation. However, addition of stoichiometric amounts of Zα causes a rapid transition to the Z-conformation. Raman spectroscopy of crystals of the Zα–$(dCrG)_3$ complex confirm that the chimeric oligonucleotide is stabilized in the Z-conformation. A complete data set has been obtained at 2.5 Å resolution. The Zα–$(dCrG)_3$ crystals belong to the tetragonal *I*422 space group, with unit-cell parameters $a = b = 104.2$, $c = 117.6$ Å. Work is under way to solve the structure by molecular replacement.

1. Introduction

Double-stranded RNA adenosine deaminase (ADAR1) is an RNA-editing enzyme that modifies the genetic message by deaminating adenosines in double-stranded RNA; the resultant inosines are recognized as guanosines in translation. ADAR1 contains a bipartite N-terminal domain called Zab, which as well as its subdomain, Zα, binds Z-DNA with high affinity (Herbert *et al.*, 1995, 1997; Schwartz, Lowenhaupt *et al.*, 1999). A crystal structure of Zα bound to a segment of Z-DNA revealed the specific interactions of this protein with Z-DNA (Schwartz, Rould *et al.*, 1999).

ADAR1 is also thought to function in the host antiviral response. During infections by RNA viruses, interferon induces synthesis of full-length ADAR1, which accumulates in the cytoplasm of mammalian cells (Patterson & Samuel, 1995). Late in the infection it has been observed that some viral genomes contain significant numbers of A→G and U→C mutations. Such mutations are the expected result of the action of ADAR1 on the replicating viral RNA. Hypermutation has been detected during infections by measles, parainfluenza, vesicular stomatitis virus and respiratory syncytial viruses (Cattaneo, 1994; Bass, 1997). Recent studies have shown that Zα can also recognize the left-handed conformation of Z-RNA (Brown *et al.*, 2000). This result suggests that ADAR1 may utilize the Zα domain to locate areas of ongoing viral replication in the cytoplasm, facilitating hypermutation.

The left-handed Z-conformation of RNA was intensively studied after its identification in 1984 (Hall *et al.*, 1984). It has been possible to crystallize small ribo-oligonucleotides in the Z-conformation by modification of the bases (Tomita *et al.*, 1984; Nakamura *et al.*, 1985). An RNA dinucleotide embedded within a DNA segment also crystallized in the Z-conformation (Teng *et al.*, 1989).

Z-DNA is energetically unfavorable relative to B-DNA. However, Z-RNA formation is even more unfavorable compared with A-RNA, owing to the additional 2′-OH groups. Here, we examine the interaction of Zα with an RNA–DNA chimera in the Z-conformation. The use of alternating deoxyribose and ribose sugars in the backbone of $(dCrG)_3$ stabilizes the formation of Z-RNA in the presence of Zα and facilitates crystallization. We report the crystallization and preliminary diffraction results of this chimeric oligonucleotide complexed with the Zα subdomain of human ADAR1. This result is the first example of the Z-conformation containing ribonucleotides specifically bound to a protein of biological interest. Additionally, this is the first example of a protein which specifically recognizes both dsRNA and dsDNA.

2. Materials and methods

2.1. Protein and nucleic acid purification and preparation

Recombinant Zα protein (residues L133–G209 of human ADAR1) was expressed and purified as described previously (Schwartz, Lowenhaupt *et al.*, 1999). Chimeric oligonucleotides with alternating furanose sugars, $(rCdG)_3$ and $(dCrG)_3$, were obtained from

Dharmacon (Boulder, CO, USA). The oligonucleotides were deprotected using 100 m*M* *N,N,N′,N′*-tetramethylethylenediamine (TEMED) acetate pH 3.8 as described in Scaringe (2000). Following deprotection, the oligonucleotides were lyophilized, resuspended and dialyzed into 5 m*M* HEPES pH 7.5, 10 m*M* NaCl. These oligonucleotides were of sufficient purity to crystallize without further purification. Double-stranded oligonucleotides were formed by incubating solutions 1 m*M* in strands at 353 K for 10 min, then slowly cooling to 298 K in 5 m*M* HEPES pH 7.5, 100 m*M* NaCl. Annealed ds-chimeras were purified by FPLC anion-exchange chromatography as described previously (Schwartz, Shafer *et al.*, 1999).

2.2. Circular dichroism spectroscopy

Circular dichroism (CD) spectra were collected in 1 nm steps from 350 to 200 nm using an Aviv 202 spectrometer in 0.2 cm quartz cuvettes at 298 K. CD samples contained 24 µ*M* duplex chimera in 10 m*M* Na_2HPO_4 pH 7, 20 m*M* NaCl, 0.5 m*M* EDTA. Zα–chimera complexes were prepared by incubating samples 24 µ*M* in chimera duplex, 40 µ*M* in Zα (500 µl volume, a ratio of one Zα per 4 bp duplex chimera) at 298 K for 5 min, then acquiring the spectrum.

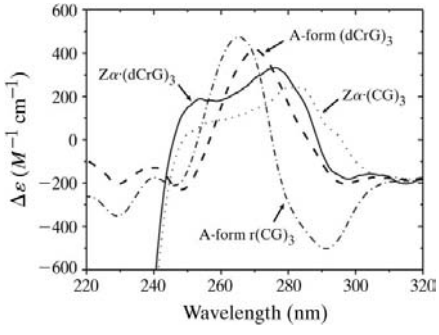

Figure 1
Circular dichroism spectra of $r(CG)_3$ and $(dCrG)_3$ in the A- and Z-conformations. In low concentrations of salt (24 µ*M* duplex oligonucleotides in 10 m*M* Na_2HPO_4 pH 7.5, 20 m*M* NaCl, 0.5 m*M* EDTA), both $r(CG)_3$ and $(dCrG)_3$ are in the A-conformation, characterized by broad positive bands centered at 266 and 270 nm, respectively. Upon the addition of Zα to 40 µ*M* (a ratio of one Zα per 4 bp) the A-conformation spectra change for both $r(CG)_3$ and $(dCrG)_3$; Zα has no CD signal above 250 nm but a strong negative ellipticity below 250 nm. Inversion of the CD bands around 285 nm for $r(CG)_3$ and 276 for $(dCrG)_3$, accompanied by decreases in the signals at 266 or 270 nm, respectively, are characteristic of the A→Z transition. It is important to note that $r(CG)_3$ requires either a prolonged incubation at 298 K or heating (*e.g.* 318 K) for the A→Z transition to occur, while the A→Z transition occurs readily at 298 K for $(dCrG)_3$.

2.3. Crystallization of the Zα–$(dCrG)_3$ complex

Purified solutions of Zα and the various oligonucleotides were concentrated to ∼1 m*M* each using centrifugal concentrators and were stored in 5 m*M* HEPES pH 7.5, 10 m*M* NaCl at 277 K as separate stocks. Zα–$(dCrG)_3$ complexes were formed by mixing a twofold excess of Zα with each duplex oligonucleotide to obtain a final concentration of 300 µ*M* complex; these mixtures were incubated at 298 K for 30 min prior to setting up crystallization trials. The hanging-drop vapor-diffusion method was employed for screening using two commercial sparse-matrix crystal screens (Hampton Research, Laguna Niguel, CA, USA). Additional screenings were performed using conditions similar to those used by Schwartz and coworkers with the Zα–Z-DNA complex (Schwartz, Shafer *et al.*, 1999). Samples of the pre-equilibrated Zα–$(dCrG)_3$ complex (2 µl) were mixed with 1 or 2 µl of reservoir solution on a siliconized glass cover slip; the crystallization mixtures were incubated at 298 K. Once conditions were established, crystals were grown using both sitting- and hanging-drop methods. Final reservoir conditions established for the Zα–$(dCrG)_3$ complex were 1.8 *M* $(NH_4)_2SO_4$ pH ≃ 5.2, 10%(*v*/*v*) glycerol.

2.4. X-ray diffraction experiments

Preliminary X-ray diffraction experiments were carried out with a MAR345 image-plate detector using Cu *K*α radiation supplied by a rotating-anode generator (Rigaku). Other experiments were carried out at beamline X12C at the National Synchrotron Light Source, Brookhaven National Laboratory. Crystals were either harvested from the mother liquor and directly flash-frozen in the liquid-nitrogen cold-stream (100 K) or were dipped in Paratone-N (Hampton Research) for a few seconds prior to flash-freezing. Complete data sets were collected from single crystals using 1° oscillations. Data were indexed and integrated using the program *MOSFLM* (Leslie, 1992). The integrated reflections were scaled, merged and truncated to obtain structure-factor amplitudes using the *CCP4* programs *SCALA* and *TRUNCATE* (Collaborative Computational Project, Number 4, 1994).

2.5. Raman spectroscopy

Raman spectra were obtained using a HoloLab series 5000R Raman microscope (Kaiser Optical Systems, Ann Arbor, MI, USA). Single crystals were mounted in 0.5 mm glass capillaries or placed directly onto the surface of a glass cover slip. Samples were irradiated at 785 nm using an argon-ion laser-pumped titanium-sapphire laser operating at 25 mW at the sample (Renova 306 C 6 W Ar ion/890 CW TiS Laser SW Lp, Coherent, Santa Clara, CA, USA). Spectra were collected using the 50× objective *via* simultaneous excitation and acquisition for 10 s; 10–15 acquisitions were averaged, corrected for cosmic rays and spectral response and the wavelength was calibrated using the spectral features of a cyclohexane standard acquired in the same manner. Calibration and baseline corrections were performed with the *Grams*5.1 program (Galactic Industries, Salem, NH, USA).

It is important to note that crystals sealed in glass or quartz capillaries were capable of X-ray diffraction at ambient temperature after performing the Raman measurements with no apparent loss of data quality. In cases where crystals are difficult to grow or material is scarce, this method permits obtaining Raman spectra and X-ray diffraction data from a single crystal.

3. Results and discussion

3.1. CD spectroscopy

Biophysical studies have shown that the Zα protein is able to induce an A→Z transition in chimeric oligonucleotides with alternating ribose and deoxyribose furanose sugars such as $(dCrG)_3$ or $(rCdG)_3$ with kinetics and activation energies similar to

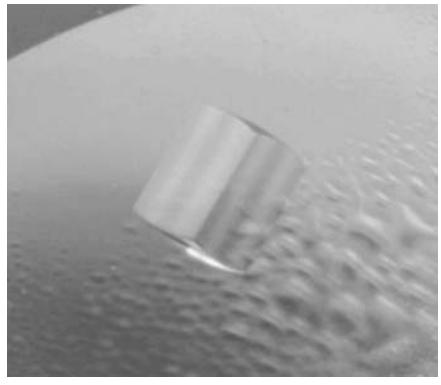

Figure 2
A crystal of the Zα–$(dCrG)_3$ complex viewed in polarized light. The tetragonal crystal (space group *I*422) was grown by hanging-drop vapor diffusion from a mother liquor created by mixing two volumes of 600 µ*M* Zα, 300 µ*M* duplex $(dCrG)_3$, 5 m*M* HEPES pH 7.5, 20 m*M* NaCl with one volume of precipitant solution containing 1.8 *M* $(NH_4)_2SO_4$ pH ≃ 5.2, 10% glycerol over a reservoir of the same precipitant. The crystal dimensions are approximately 0.8 × 0.8 × 0.8 mm.

Table 1
Data-collection and processing statistics.

Values in parentheses correspond to reflections in the highest resolution shell.

Space group	*I*422 (No. 97)
Unit-cell parameters (Å)	$a = b = 104.2$, $c = 117.6$
Resolution range (Å)	21.9–2.5
Measured reflections	83795
Unique reflections	10853
Observational redundancy	7.7
Completeness (%)	92.9 (94.7†)
R_{sym}‡ (%)	5.8 (50.3)
$I/\sigma(I)$	8.5 (1.5)

† Completeness in the outermost shell is higher than the overall completeness owing to incompleteness in the lowest resolution shell (∞–7.8 Å, 84.1%). ‡ $R_{sym} = \sum\sum|I(h)_i - \langle I\rangle|/\sum\langle I(h)\rangle$, where $I(h)$ is the observed intensity of the ith measurement of reflection h and $\langle I(h)\rangle$ is the mean intensity of reflection h.

those of DNAs of the same sequence (B. A. Brown II, manuscript in preparation). In contrast, A→Z transitions for native RNAs of the same sequence, *i.e.* $r(CG)_3$, have markedly slower kinetics and higher activation energies (Brown *et al.*, 2000). These results indicated that the chimeric oligonucleotides required less energy to form stable complexes with Zα than RNA oligonucleotides and may be appropriate RNA analogs for crystallization.

Circular dichroism spectroscopy was used to ensure that all sequences used for crystallization trials are stabilized in the Z-conformation by Zα. Fig. 1 shows the CD spectra of $(dCrG)_3$ in the A-conformation and stabilized in the Z-conformation after addition of Zα. The corresponding spectra of $r(CG)_3$ are shown for comparison. In the presence of one molecule of Zα per 4 bp (24 µ*M* 6-mer duplex, 40 µ*M* Zα), both oligonucleotides exhibit characteristic spectral changes. The Zα–$(dCrG)_3$ spectrum is clearly distinguishable from the A-conformation spectrum and is characteristic of the spectra of left-handed nucleic acids. These results are in good agreement with those reported previously (Brown *et al.*, 2000).

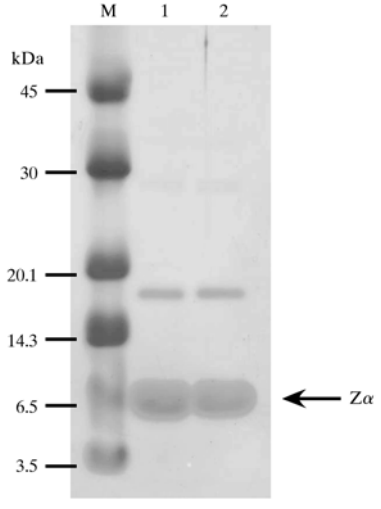

Figure 3
The presence of Zα protein in the crystals was verified by SDS–PAGE. Samples of the crystallization setup mixture of the protein and nucleic acid and a dissolved Zα–$(dCrG)_3$ crystal are compared. Lane 1, molecular-weight markers; lane 2, crystal setup solution; lane 3, dissolved Zα–$(dCrG)_3$ complex.

3.2. Crystallization results

We were able to co-crystallize Zα with the chimeric sequence $(dCrG)_3$. Crystals of this complex grew from a mother liquor consisting of 1.8 *M* ammonium sulfate and 10%(*v*/*v*) glycerol at 298 K. Single crystals were visible approximately 3 d after setup and reached their maximal size after 9–12 d (Fig. 2). It is interesting to note that although a full screen for crystallization conditions was performed, the final conditions were nearly identical to those used for the Zα–$dT(CG)_3$ complex, even though the chimeric sequence is lacking the 5′-terminal thymidine (Schwartz, Shafer *et al.*, 1999). In comparison, the Zα–$(rCdG)_3$ crystals were cube-shaped and differed from the long rods obtained by Schwartz and coworkers with Zα–$dT(CG)_3$ (Schwartz, Shafer *et al.*, 1999).

The presence of Zα protein in the crystals was verified by performing SDS–PAGE on dissolved crystals (Fig. 3). The existence of nucleic acid in Zα–$(rCdG)_3$ crystals was established by dissolving a single crystal in water and then obtaining a UV absorbance spectrum; a strong absorbance peak at 260 nm indicated the presence of nucleic acid, in addition to an absorbance at 280 nm contributed by the Zα protein. Related sequences, such as $r(CG)_3$ and $(rCdG)_3$ failed to produce crystals under the conditions tested. We attribute the success with $(dCrG)_3$ to the alteration of the furanose sugars. In the Z-conformation, guanosine residues adopt the *syn*-glycosyl orientation with 3′-*endo* sugar puckers, while cytidines are in the *anti*-glycosyl orientation with 2′-*endo* sugar puckers. It takes significantly more energy to change the pucker of a ribose sugar compared with deoxyribose (Olson & Sussman, 1982; Sanger, 1984). The chimeric oligonucleotide $(dCrG)_3$ is designed to favor alternating sugar puckers in the Z-conformation compared with a completely ribose oligonucleotide, which would disfavor the 2′-*endo* conformation in the cytidine riboses. The $(dCrG)_3$ oligonucleotide forms a more stable Z-conformation and reduces the energy necessary to bring about the A→Z-form transition. This interpretation is further supported by the fact that the few crystals obtained of Zα complexed with $rU(CG)_3$ did not diffract well, suggesting that they had poor internal order. This inherent disorder is presumably a reflection of the higher energy requirements of maintaining a pure RNA in the Z-conformation.

3.3. Raman spectroscopy

Raman spectra were obtained on crystals of the Zα–$(dCrG)_3$ complex in order to evaluate the conformation of the oligonucleotide in the complex prior to performing detailed crystallographic analysis. The Raman spectrum of the Zα–$(dCrG)_3$ crystals (Fig. 4) had an intense peak at 980 cm^{-1} and a lesser peak at 455 cm^{-1} which correspond to vibrations arising from $(NH_4)_2SO_4$ in the mother liquor. Features pertinent to conformation of the nucleic acid are found in the 500–800 cm^{-1} region of the spectrum. The band at 786 cm^{-1} arises from cytosine ring breathing and phophodiester stretching vibrations from the backbone. The presence of a band at around 636 cm^{-1} is the most notable indication that the $(dCrG)_3$ oligonucleotide in these crystals is in the Z-conformation (Benevides & Thomas, 1983). This mode is attributable to riboguanosine residues in the *syn*-glycosyl

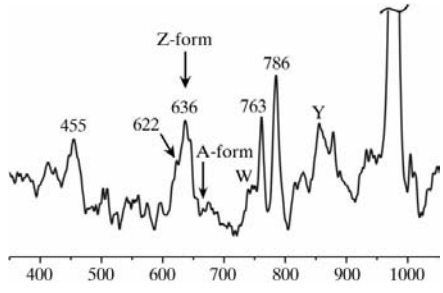

Figure 4
Raman spectroscopy of Zα–$(dCrG)_3$ complex crystals. Raman signals in the 500–800 cm^{-1} region provide useful information about the conformation of the nucleic acid in the complex. The band at 786 cm^{-1} is a composite of two vibrations, a cytidine ring breathing-mode and phosphodiester backbone stretching; this band is relatively insensitive to the RNA conformation. In contrast, the mode at 636 cm^{-1} is indicative of guanosine in the *syn*-glycosyl orientation with a 3′-*endo* sugar pucker and can be considered diagnostic of the Z-conformation of RNA (indicated Z-form). This mode is near a phenylalanine band at 622 cm^{-1} arising from the Zα protein. The mode at 763 cm^{-1} arises from tryptophan ring vibrations from the Zα protein. Additional bands assignable to tyrosine are also indicated. The intense band at 980 cm^{-1} and the lesser band at 455 cm^{-1} are from $(NH_4)_2SO_4$ in the precipitant. Absence of an intense mode at 668 cm^{-1}, indicative of the A-conformation of RNA, is also indicated.

orientation with 3′-*endo* sugar puckers. In A-RNA, riboguanosines in the familiar *anti*-glycosyl orientation with 3′-*endo* sugar puckers have a Raman band near 668 cm^{-1} (Benevides & Thomas, 1983). We conclude from these results that the $(dCrG)_3$ oligonucleotide is in the Z-conformation. The 600–800 cm^{-1} spectral region has several features similar to those seen with solution Raman measurements of poly(rG-dC)–poly(rG-dC) in the Z-conformation which was induced by high concentrations of salt (Wu & Behe, 1984). A fairly intense mode at 763 cm^{-1} arises from the tryptophan ring vibration, as seen in the Zα–$r(CG)_6$ solution Raman measurements (Brown *et al.*, 2000). Bands are also seen for phenylalanine vibrations in the 800–900 cm^{-1} region.

3.4. Diffraction results

X-ray diffraction data were obtained for native crystals using both rotating-anode and synchrotron radiation at 100 K. The Zα–$(dCrG)_3$ crystals typically diffracted to a maximum resolution of 2.5 Å and there was not significant improvement in the synchrotron data compared with data collected on the rotating anode. The crystal has been assigned to the tetragonal space group *I*422, with unit-cell parameters $a = b = 104.2$, $c = 117.6$ Å. A full data set has been collected and the results from processing are shown in Table 1. The data are of sufficiently good quality to proceed with a molecular-replacement solution of this structure using the Zα–Z-DNA complex of Schwartz and coworkers as a model (Schwartz, Rould *et al.*, 1999; PDB accession number 1qbj). A comparison of the Zα–Z-chimera crystals with those obtained with Zα–$dT(CG)_3$ reveals several differences. Although both have tetragonal space groups, the Zα–$(dCrG)_3$ crystals belong to space group *I*422 and the Zα–Z-DNA crystals to $P42_12$, with unit-cell parameters $a = b = 85.9$, $c = 71.3$ Å (Schwartz, Shafer *et al.*, 1999). We expect that the Zα–Z-chimera crystals contain the same number of complexes in the asymmetric unit as the Zα–$dT(CG)_3$ crystals.

This work was supported by grants to AR from the NIH and NSF. BAB was supported by an Aid for Cancer Research Postdoctoral Fellowship. AA is supported by a Human Frontiers Science Program long-term fellowship. Raman microscopy was performed at the MIT Center for Materials Science and Engineering Analytical Shared Experimental Facility, which is supported by the National Science Foundation. Special thanks to Tim McClure and Dr Martin Hunter (MIT) for assistance with the Raman microscopy. Crystallographic data collection was performed at Beamline X12C, the National Synchrotron Light Source, Brookhaven National Laboratory. EBH is supported by a grant from the Office of Research and Development, Medical Research Service, Department of Veterans Affairs.

References

Bass, B. L. (1997). *Trends Biochem. Sci.* **22**, 157–162.
Benevides, J. M. & Thomas, G. J. (1983). *Nucleic Acids Res.* **11**, 5747–5761.
Brown, B. A. II, Lowenhaupt, K., Wilbert, C. M., Hanlon, E. B. & Rich, A. (2000). *Proc. Natl Acad. Sci. USA*, **97**, 13532–13536.
Cattaneo, R. (1994). *Curr. Opin. Genet. Dev.* **4**, 895–900.
Collaborative Computational Project, Number 4 (1994). *Acta Cryst.* D**50**, 760–763.
Hall, K., Cruz, P., Tinoco, I. Jr, Jovin, T. M. & van de Sande, J. H. (1984). *Nature (London)*, **311**, 584–586.
Herbert, A., Alfken, J., Kim, Y. G., Mian, I. S., Nishikura, K. & Rich, A. (1997). *Proc. Natl Acad. Sci. USA*, **94**, 8421–8426.
Herbert, A., Lowenhaupt, K., Spitzner, J. & Rich, A. (1995). *Proc. Natl Acad. Sci. USA*, **92**, 7550–7554.
Leslie, A. G. W. (1992). *Jnt CCP4/ESF–EAMCB Newsl. Protein Crystallogr.* **26**.
Nakamura, Y., Fujii, S., Urata, H., Uesugi, S., Ikehara, M. & Tomita, K. (1985). *Nucleic Acids Symp. Ser.* **16**, 29–32.
Patterson, J. B. & Samuel, C. E. (1995). *Mol. Cell Biol.* **15**, 5376–5388.
Olson, W. K. & Sussman, J. L. (1982). *J. Am. Chem. Soc.* **104**, 207–278.
Sanger, W. (1984). *Principles of Nucleic Acid Structure*, edited by C. R. Cantor. New York: Springer-Verlag.
Scaringe, S. A. (2000). *Methods Enzymol.* **317**, 3–18.
Schwartz, T., Lowenhaupt, K., Kim, Y. G., Li, L., Brown, B. A. II, Herbert, A. & Rich, A. (1999). *J. Biol. Chem.* **274**, 2899–2906.
Schwartz, T., Rould, M. A., Lowenhaupt, K., Herbert, A. & Rich, A. (1999). *Science*, **284**, 1841–1845.
Schwartz, T., Shafer, K., Lowenhaupt, K., Hanlon, E., Herbert, A. & Rich, A. (1999). *Acta Cryst.* D**55**, 1362–1364.
Teng, M. K., Liaw, Y. C., van der Marel, G. A., van Boom, J. H. & Wang, A. H. (1989). *Biochemistry*, **28**, 4923–4928.
Tomita, K., Nakamura, Y., Nishikura, K., Fujii, S., Uesugi, S. & Ikehara, M. (1984). *Acta Cryst.* A**40**(Suppl.), C45.
Wu, H. Y. & Behe, M. J. (1984). *Proc. Natl Acad. Sci. USA*, **81**, 7284–7287.